

Time-resolved observation of fast hotspot dynamics in superconducting nanowires

M. Ejrnaes,^{1,*} A. Casaburi,¹ F. Mattioli,² R. Leoni,² S. Pagano,^{1,3} and R. Cristiano¹

¹Istituto di Cibernetica “E. Caianiello” del CNR, 80078 Pozzuoli, Italy

²Istituto di Fotonica e Nanotecnologie del CNR, 00156 Roma, Italy

³Dipartimento di Matematica e Informatica and Istituto SPIN del CNR-Salerno, Università di Salerno, 84084 Fisciano, Italy

(Received 31 December 2009; revised manuscript received 4 March 2010; published 23 April 2010)

We present time-resolved measurements of fast hotspots in superconducting nanowires that allow a direct visualization of the hotspot evolution. The measurements were made possible exploiting an innovative parallel nanowire configuration. We measure that the hotspot lifetime is independent of bias current and hotspot width. We observe that the hotspot expansion is slower than its relaxation and that a time delay on the order of 1 ns occurs between the maximum hotspot power dissipation and maximum hotspot expansion rate. The time delay was found to increase with increasing bias current and it decreases slightly for wider hotspots. On the basis of the observed dynamic evolution, we argue that the hotspot expands rapidly when the temperature gradient on the hotspot boundary is low, and that it expands slowly when this gradient is large.

DOI: [10.1103/PhysRevB.81.132503](https://doi.org/10.1103/PhysRevB.81.132503)

PACS number(s): 74.40.Gh, 74.78.-w, 85.25.Oj

Current-carrying superconductors can be in two stable states when the transport current is sufficiently high. The bistability is related to the presence of localized normal domains within the superconductor, called *hotspots*, where the current causes Joule self-heating. Many aspects related to the presence of hotspots in superconductors have been investigated both theoretically and experimentally.¹ Hotspots also appear in superconducting thin films and their static properties have been investigated and observed experimentally²⁻⁴ but their dynamic properties have received less attention. This is unfortunate since two high-performance detectors, the superconducting hot-electron mixer⁵ and the superconducting nanowire single-photon detector (SNSPD),⁶ are based on the dynamic properties of such hotspots. In fact, the two applications exploit different types of hotspots. The mixer uses the very fast change in size of a *stable* hotspot whereas the SNSPD uses the fast and sensitive generation of an *unstable* hotspot.⁷ Currently, the best realizations of these detectors are based on hotspots in ultrathin NbN films. Some insight into the dynamic properties of unstable hotspots in ultrathin NbN nanowires was recently obtained by measuring the stability of unstable hotspots.⁸ To properly describe the measured stability a delay, on the order of 1 ns, between the Joule heating and the hotspot expansion was added to the standard theory of domain-wall movement.¹

Here we present time-resolved measurements of fast unstable hotspots in ultrathin NbN nanowires. They provide a direct visualization of the temporal evolution of the hotspot. We also observe a time delay between the peak in the power dissipation and the peak in the resistance change in agreement with Ref. 8. On the basis of the observed dynamic evolution, we will argue that the hotspot expands faster when the temperature gradient on the hotspot boundary is low than when this gradient is large.

The hotspot time evolution in ultrathin NbN nanowires is fast and is most conveniently measured through the time dependence of its electrical resistance, $R(t)$. To follow the fast dynamics and obtain time-resolved information, a high bandwidth connection is required. This connection will shunt the superconductor, thereby providing an electrothermal feedback, and makes it possible to study unstable hotspots in

a repeatable and controlled way. Therefore, the unstable hotspots studied in this work are effectively embedded in an electric circuit [see Fig. 1(a)] that we model in a standard way,⁸ taking into account the total inductance in the circuit, L , the load impedance, Z , and the dc current bias, I_0 . From the circuit equations, the $R(t)$ and its time derivative, $\dot{R}(t)$, can be calculated as

$$R = \frac{V + \dot{V}L/Z}{I_0 - V/Z}, \quad \dot{R} = \frac{\dot{V}(R+Z) + \ddot{V}L}{ZI_0 - V}, \quad (1)$$

where $V(t)$ is the measured voltage signal. From Eq. (1), we can obtain $R(t)$ having $V(t)$, $\dot{V}(t)$, along with good values of L and Z . Furthermore, to obtain $\dot{R}(t)$, we also need $\ddot{V}(t)$. We note that some qualitative insight into the dynamical behavior of the unstable hotspot can be obtained by examining the instant when $V(t)$ reaches its maximum. Since $\dot{V}(t)=0$ at the maximum at this time instant, R can be obtained directly from Eq. (1) using only Z . Furthermore, at this point, in time

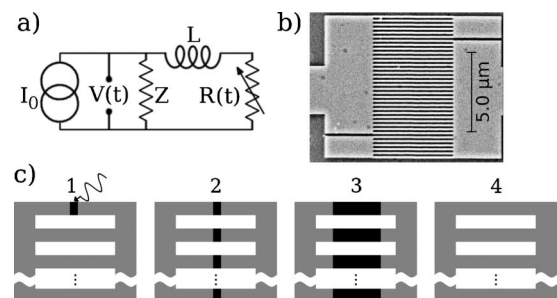


FIG. 1. (a) The electric circuit used in the measurements and also to calculate $R(t)$. (b) Scanning electron micrograph of the device based on 24 parallel nanowires. (c) Sketch showing the temporal evolution of the *unstable* hotspot (black regions) that occurs in the parallel nanowires (shown in gray). 1: a photon absorption event induces a hotspot in a nanowire. 2: hotspots nucleate in all parallel nanowires through a cascade switch and the signal voltage starts to appear. 3: the hotspots expand. 4: superconductivity is restored in the parallel nanowires.

$\dot{R} < 0$ because $\ddot{V} < 0$. So, when $V(t)$ reaches its maximum, the hotspot should still be present with a decreasing resistance. For this reason, the maximum of $R(t)$ should always occur before $V(t)$ reaches its maximum.

One can use the extreme energy sensitivity of ultrathin NbN nanowires to externally induce the hotspot with a minimal influence on the subsequent Joule-heating-induced dynamics. In fact, unstable hotspots in narrow ultrathin NbN nanowires can be induced using single photons of 0.5 eV. However, $R(t)$ is difficult to obtain because the hotspot evolution is very fast⁹ and the signal-to-noise ratio is low. In this work, we have used a parallel configuration of nanowires to significantly increase the measured signal-to-noise ratio.¹⁰ The advantage is that a single photon induces a hotspot in each of the parallel nanowires through a cascade switch mechanism. Furthermore, we have inserted an external inductance to extend the hotspot lifetime to a few nanoseconds.^{11,12} With this technique, we are able to perform accurate measurements of $V(t)$ which allows us to numerically calculate both $\dot{V}(t)$ and $\ddot{V}(t)$ to obtain $R(t)$ and $\dot{R}(t)$.

Ultrathin NbN nanowires with a thickness of 9 nm and a width of 100 nm were used to fabricate four types of devices. The devices were based on either 4, 8, 12, or 24 parallel nanowires, respectively [this last type is shown in Fig. 1(b)]. During the measurement, the devices nucleate a hotspot in all the parallel nanowires when a photon is absorbed in any one of them.¹¹ Therefore, we measure the combined effect of several hotspots in parallel [as shown in Fig. 1(c)], which effectively form a *composite* hotspot with an equivalent width proportional to the number of parallel wires. For simplicity, we will discuss the measurements in terms of the composite hotspot in this work. Due to the different number of parallel nanowires, the fabricated devices had composite hotspot widths of 400 nm, 800 nm, 1.2 μm , and 2.4 μm . During the measurements, the devices were operated with an extra in series 470 nH inductor which ensures that no current leaks out to the load during the cascade switch. The devices were polarized with a dc current, using battery powered electronics, through a low-temperature low-pass filter and a coaxial cable provided the high bandwidth connection. The presence of an unstable hotspot created a signal pulse which was amplified by room-temperature rf amplifiers and digitized using either a 1 GHz bandwidth sampling oscilloscope or a 9 GHz bandwidth oscilloscope. In the measurements, the oscilloscope was triggered on the signal pulse in order to avoid timing errors in the generation of the hotspot.¹³ We induce hotspot formation by exposing the devices to weak laser-light pulses through an optical window in the cryostat. The laser-pulse repetition rate was kept low enough to allow for a complete thermalization of the devices between successive unstable hotspot formations. During all the measurements, the device temperature was 5 K. The device was mounted in vacuum and cooled through a cold finger with a large thermal mass to ensure that the observed dynamical features are not related to dynamical changes in the cooling of the superconductor.^{14–16} To get very low noise signals, we record averaged signal pulses for various values of bias current for each device. We did this with both oscilloscopes. The recorded signal pulses were identical, indicating that the sig-

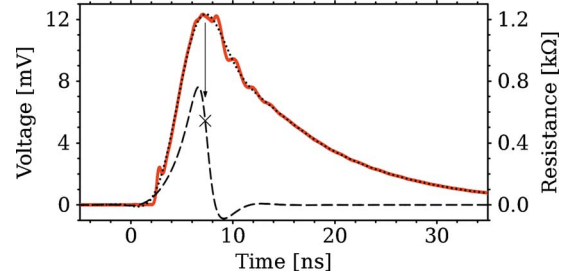


FIG. 2. (Color online) $V(t)$ (red solid line, left axis), filtered $V(t)$ (black dotted line, left axis), and calculated hotspot resistance, $R(t)$ (dashed line, right axis) for the 2.4- μm -wide hotspot at $I_0 = 255 \mu\text{A}$.

nal pulses are temporally well resolved also with the sampling oscilloscope. Since the signal pulses recorded with the sampling oscilloscope had a lower noise level, these data will be used in the remainder of this Brief Report. The averaged signal pulses show a sufficiently low noise level (see Fig. 2) but they are disturbed by a spurious resonance in the external inductance. Since the resonance is easily identifiable in the Fourier transform, we attenuate its influence on the signal pulses using an optimal filter.

In order to obtain $R(t)$ from the signal pulses, we separately determine Z and the ratio L/Z . The circuit time constant, L/Z , was measured using the fall time of $V(t)$ for each device¹⁷ and we determine Z from the following considerations. In our measurement, Z is given by the characteristic impedance of the coaxial cable. From the signal pulse amplitude, we find that Z cannot be lower than 52 Ω , as this would make the current flowing through Z larger than I_0 , which is not possible. Likewise, Z cannot exceed 55 Ω because this would create reflected signal pulses with an amplitude larger than our signal baseline noise, which we do not observe. Then we choose $Z = 53 \Omega$ and we have verified that all the results presented in this work do not depend on the exact value of Z within the range 52–55 Ω .

A representative example of a filtered $V(t)$ and the calculated $R(t)$ are shown in Fig. 2. In agreement with the qualitative result, when V reaches its maximum R is still finite, decreasing and has already passed through its maximum. R is nonzero for about 7 ns and it increases slower than it decreases. It is important to reserve attention to the uncertainty, $\sigma(R)$, of the obtained value of $R(t)$. To do that we have performed a careful investigation of the error in the voltage, $\sigma(V)$, and its time derivative, $\sigma(\dot{V})$, that contribute to $\sigma(R)$. From our analysis, it appears that the spurious oscillation in the external inductance dominates and gives rise to a $\sigma(\dot{V})$ ranging between 100 and 500 $\mu\text{V}/\text{ns}$ that mainly affects $\sigma(R)$ in the region where $R(t)$ decreases. The error analysis can explain the unphysical negative R , that occurs after R has rapidly decreased. In fact, we have found that $R + \sigma(R) > 0$ on the entire temporal scale.

In Fig. 3, we show $R(t)$ at various I_0 for two different devices. It is seen that the measurements confirm the common assumption that the initial hotspot growth is close to exponential in time for all bias currents. Also, the hotspot collapse is faster than the growth for all I_0 , in agreement with

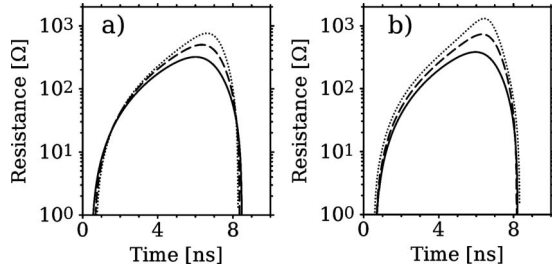


FIG. 3. (a) $R(t)$ for I_0 of 205 μA (solid line), 235 μA (dashed line), and 255 μA (dotted line) for the 2.4- μm -wide hotspot. (b) $R(t)$ for bias currents of 29 μA (solid line), 34 μA (dashed line), and 39 μA (dotted line) for the 400-nm-wide hotspot.

model results based on thermal diffusion.⁹ Furthermore, the duration of the unstable hotspot does not depend on I_0 . Almost identical dynamical behaviors are also observed for different hotspot widths, as can be seen from the 400-nm-wide hotspot in Fig. 3(b). In all the measurements, we obtain a maximum R of about 1 k Ω at high I_0 , independently of the hotspot width. This corresponds to a maximum hotspot length of 0.59 μm and 3.5 μm for the devices based on 4 and 24 parallel nanowires, respectively. As expected, these values do not exceed the nanowire length of 5.2 μm .

We have investigated if the obtained $\dot{R}(t)$ (see Fig. 4) can be described by the standard theory of domain-wall movement.^{1,8} In this theory, the temperature-dependent Joule-heating determines the velocity of the hotspot boundary as $\dot{R} = [(I_0 - V/Z)^2 - I_{ss}^2] / \gamma$,¹⁸ assuming that the temperature profile in the boundary zone does not change in time. Here I_{ss} and γ depend only on material constants and equilibrium temperature. Our observations contrast with the prediction of the theory because the initial \dot{R} increases slowly when V is low; also the maximum of \dot{R} occurs when V is close to maximum; and finally our data would require different values of I_{ss} and γ at different I_0 to properly describe the time instant when $\dot{R} = 0$.

We now turn to the relation between \dot{R} and the power dissipated in the hotspot, $P(t) = (V + \dot{V}L/Z)(I_0 - V/Z)$. As can be seen in Fig. 4, we observe a time delay, t_d between the maximum of $P(t)$ and the maximum of $\dot{R}(t)$ in good agree-

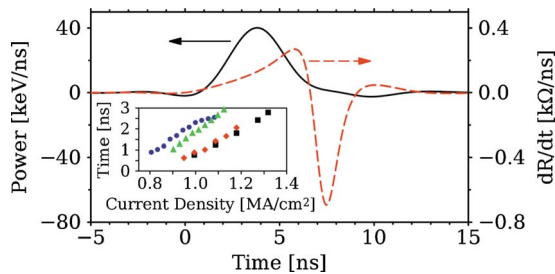


FIG. 4. (Color online) $P(t)$ (solid black line, left axis) and $\dot{R}(t)$ (dashed red line, right axis) for the 2.4- μm -wide hotspot at $I_0 = 255 \mu\text{A}$. Inset: t_d vs bias current density for the 400 nm (blue circles), 800 nm (green triangles), 1.2 μm (black squares), and 2.4 μm (red diamonds) wide hotspots.

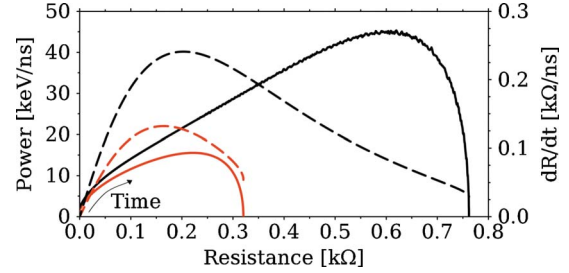


FIG. 5. (Color online) $P(t)$ (dashed lines, left axis) and $\dot{R}(t)$ (solid lines, right axis) vs $R(t)$ at $I_0 = 205 \mu\text{A}$ (red lines) and 255 μA (black lines) for the 2.4- μm -wide hotspot.

ment with Ref. 8. t_d was found to increase roughly linearly with increasing I_0 . This is shown in the inset of Fig. 4, where we show t_d as a function of the bias current density to compare the results obtained with different devices. This comparison shows that t_d tends to be slightly shorter for wider hotspots at the same current density.

With the available information, we can investigate what causes the observed delay. To this end, it is useful to plot $P(t)$ versus $R(t)$ (see Fig. 5), for a low and a high I_0 . Here we see that the peak in P occurs in a narrow range of R around 175 Ω , indicating that it occurs in a hotspot of constant volume, independently of I_0 . We also show $\dot{R}(t)$ versus $R(t)$. It is seen that the maximum of $\dot{R}(t)$ occurs in a much larger range of R . It is seen that an increased P makes the hotspot expand to a much larger volume before the peak in $\dot{R}(t)$ occurs. As shown in the inset of Fig. 4, this also increases t_d . In brief, the maximum \dot{R} occurs later and in a larger volume at a higher I_0 .

We think these observations show that \dot{R} is dependent on both P and the temperature gradient in the hotspot boundary zone. In particular, the dependence on the gradient is so strong that the hotspot expands most rapidly when the gradient is low. Within the hypothesis of a strong dependence on the temperature gradient, the observed increase in t_d with I_0 occurs because the hotspot volume absorbing the peak P is roughly the same. An increased P will create a steeper gradient in the hotspot boundary zone, which in turn will take a longer time to decrease and make t_d longer. We note that the rapid decrease in R is consistent with a temporally decreasing thermal gradient in the hotspot boundary zone because superconductivity is restored almost simultaneously in the entire hotspot volume. The presented experiments cannot determine the physical origin of the fast boundary movement with a low-temperature gradient in the hotspot boundary zone. It is possible that a low-temperature gradient could reduce the energy needed to destroy superconductivity in the region adjacent to the hotspot boundary through a temperature increase. Alternatively, if it takes a finite amount of time to suppress the superconducting order parameter adjacent to the hotspot boundary, as in the case of applied supercritical currents,^{13,19} this time could be reduced in the presence of a low-temperature gradient.

In conclusion, detailed insight into the dynamics of unstable hotspots in ultrathin NbN wires has been achieved

through fast low noise measurements. The hotspot lifetime was constant independently of bias current and hotspot width. Likewise, the hotspot expansion was slower than the collapse for all bias currents and hotspot widths. In agreement with a recent hypothesis, we observe a time delay on the order of 1 ns between the maximum power dissipated in the hotspot and its maximum expansion speed. The time delay was found to increase with increasing bias current and it decreases slightly for wider hotspots. On the basis of the

observed dynamic evolution, we argue that the hotspot expansion is strongly influenced by the temperature gradient on the hotspot boundary. The hotspot expands rapidly when the gradient is low and slowly when it is large. Further work is needed to determine which physical mechanisms are responsible. In any case, we believe that experiments like those described here will be useful measurement tools in future work for time-resolved investigations of hotspot dynamics in other material systems.

*m.ejrnaes@cib.na.cnr.it

¹A. V. Gurevich and R. G. Mints, *Rev. Mod. Phys.* **59**, 941 (1987).

²W. J. Skocpol, M. R. Beasley, and M. Tinkham, *J. Appl. Phys.* **45**, 4054 (1974).

³S. Yamasaki and T. Aomine, *Jpn. J. Appl. Phys.* **18**, 667 (1979).

⁴D. Doenitz, R. Kleiner, D. Koelle, T. Scherer, and K. F. Schuster, *Appl. Phys. Lett.* **90**, 252512 (2007).

⁵Planned for use on the Herschel Space Observatory [S. Cherednichenko, V. Drakinskiy, T. Berg, P. Khosropanah, and E. Kollberg, *Rev. Sci. Instrum.* **79**, 034501 (2008)]; and the Stratospheric Observatory for Infrared Astronomy (experiments CASIMIR and GREAT, available online <http://www.sofia.usra.edu/>).

⁶R. H. Hadfield, *Nat. Photonics* **3**, 696 (2009).

⁷In this paper, we will use *unstable* to describe a hotspot that will collapse after a certain time; a hotspot that will remain present when created is *stable*.

⁸A. J. Kerman, J. K. W. Yang, R. J. Molnar, E. A. Dauler, and K. K. Berggren, *Phys. Rev. B* **79**, 100509(R) (2009).

⁹J. K. W. Yang, A. J. Kerman, E. A. Dauler, V. Anant, K. M.

Rosfjord, and K. K. Berggren, *IEEE Trans. Appl. Supercond.* **17**, 581 (2007).

¹⁰M. Ejrnaes, R. Cristiano, O. Quaranta, S. Pagano, A. Gaggero, F. Mattioli, R. Leoni, B. Voronov, and G. Goltsman, *Appl. Phys. Lett.* **91**, 262509 (2007).

¹¹M. Ejrnaes, A. Casaburi, O. Quaranta, S. Marchetti, A. Gaggero, F. Mattioli, R. Leoni, S. Pagano, and R. Cristiano, *Supercond. Sci. Technol.* **22**, 055006 (2009).

¹²K. Suzuki, S. Miki, S. Shiki, N. Zen, Z. Wang, and M. Ohkubo, *Physica C* **469**, 1677 (2009).

¹³M. Ejrnaes *et al.*, *Appl. Phys. Lett.* **95**, 132503 (2009).

¹⁴Y. Iwasa and B. A. Apgar, *Cryogenics* **18**, 267 (1978).

¹⁵Y. M. Lvovsky and M. O. Lutset, *Cryogenics* **22**, 581 (1982).

¹⁶I. Funaki, F. Irie, M. Takeo, U. Ruppert, I. Luders, and G. Klipping, *Cryogenics* **25**, 139 (1985).

¹⁷A. J. Kerman, E. A. Dauler, W. E. Keicher, J. K. W. Yang, K. K. Berggren, G. Goltsman, and B. Voronov, *Appl. Phys. Lett.* **88**, 111116 (2006).

¹⁸In our case, the domain-wall velocity is proportional to \dot{R} .

¹⁹M. Tinkham, *Nonequilibrium Superconductivity, Phonons, and Kapitza Boundaries* (Plenum, New York, 1981), pp. 231–262.